IOP Publishing Journal of Physics A: Mathematical and Theoretical

J. Phys. A: Math. Theor. **50** (2017) 084001 (17pp) doi:10.1088/1751-8121/aa5204

First passage time statistics for two-channel diffusion

Aljaž Godec[1,2,3] **and Ralf Metzler**[1]

[1] Institute of Physics & Astronomy, University of Potsdam, 14476 Potsdam-Golm, Germany
[2] Department of Molecular Modeling, National Institute of Chemistry, 1000 Ljubljana, Slovenia

E-mail: agodec@uni-potsdam.de

Received 8 August 2016, revised 30 November 2016
Accepted for publication 6 December 2016
Published 17 January 2017

Abstract

We present rigorous results for the mean first passage time and first passage time statistics for two-channel Markov additive diffusion in a 3-dimensional spherical domain. Inspired by biophysical examples we assume that the particle can only recognise the target in one of the modes, which is shown to effect a non-trivial first passage behaviour. We also address the scenario of intermittent immobilisation. In both cases we prove that despite the perfectly non-recurrent motion of two-channel Markov additive diffusion in 3 dimensions the first passage statistics at long times do not display Poisson-like behaviour if none of the phases has a vanishing diffusion coefficient. This stands in stark contrast to the standard (one-channel) Markov diffusion counterpart. We also discuss the relevance of our results in the context of cellular signalling.

Keywords: first passage time, Markov additive processes, Fokker–Planck equation, random search processes, coupled initial boundary value problem, cellular signalling, asymptotic analysis

(Some figures may appear in colour only in the online journal)

1. Introduction

When does a stochastic variable reach a preset threshold (e.g. a physical target or a given asset value) for the first time? This generic first passage time (FPT) problem [1, 2] is central to the kinetics across many disciplines, such as diffusion controlled chemical reactions [3], signalling

[3] This article belongs to the special issue: Emerging Talents, which features invited work from the best early-career researchers working within the scope of *J. Phys. A*. This project is part of the Journal of Physics series' 50th anniversary celebrations in 2017. Aljaz Godec was selected by the editorial board of *J. Phys. A* as an emerging talent.

cascades in biological cells [4–10], transport in disordered media [12] including the breakthrough dynamics in hydrological aquifers [13], the location of food by foraging bacteria and animals [14], up to the global spreading of diseases [15, 16] or stock market dynamics [17].

Despite their diverse phenomenology and owing to the central limit theorem, the kinetics in stochastic systems such as the above can often be mapped onto a standard Markovian random walk. Here we will discuss the FPT behaviour in the context of a particle diffusing in space. In open domains the FPT statistics of the random walk—or its diffusion limit—decay as a power law[4], giving rise to a diverging mean FPT (MFPT) [1]. Heavy tails are common when it comes to persistence properties of infinite systems [18]. A finite domain size, however, introduces an exponential long time decay and thus a finite MFPT, which becomes a function of the system size and dimensionality [1, 9–11, 19]. In unbounded domains all first passage trajectories are nominally *direct* [10], whereas in confinement a particle can arrive at the target site also via reflection with the confining boundary, i.e. via an *indirect* trajectory [10]. Moreover, the MFPT for non-recurrent and translation invariant Markov dynamics is often strongly dominated by the long time behaviour—by *indirect* trajectories [10, 19]. This is the case when the volume of the domain tends to be very large and/or the target size tends to be very small [19]. In such non-recurrent scenarios knowing the MFPT fully—yet non-trivially— characterises the long time asymptotic of the FPT statistics [10, 19]. In non-recurrent systems with strongly broken translation invariance an additional time scale emerges, mirroring brief excursions away from the target [10]. This intermediate time scale in turn significantly contributes to the MFPT [10]. Conversely, for recurrent motion the rate of the long time exponential decay is strongly affected by both, direct and indirect trajectories [19].

Often the dynamics additionally depend on some internal state, such as for example in the so-called 'intermittent search model', where the particle randomly switches between passive diffusion and active ballistic motion in a Poissonian [20–23] or Lévy [24] fashion, or equivalently in the 'facilitated diffusion model of gene regulation' [25], where the particle switches between 3-dimensional and 1-dimensional diffusion, with an additional dynamical component due to conformational dynamics of DNA [26], which in the annealed limit gives rise to Lévy flights [27]. A similar case is the transitioning between search and recognition modes in the 1-dimensional search of transcription factors along DNA [28].

A similar random transitioning occurs in stochastically gated chemical reactions [7, 29] and stochastically gated narrow escape [6, 7]. The Markovian switching between the internal states introduces a much richer phenomenology and can lead to qualitative changes in the FPT statistics, such as in the case of the random search for a stochastically gated target [29]. Conversely, by combining recurrent and non-recurrent motion phases and thereby suppressing oversampling on large spatial scales and improving the hitting on small length-scales, one can improve stochastic search processes in the sense of minimising the MFPT to reach the target [20, 21, 25].

From a mathematical point of view all these compound processes are called *Markov additive* (MA) [30]. MA processes are a class of Markov processes, whose state space $G = \Omega \times F$ is at least 2-dimensional and can be split into Ω, a Markovian component and an additive component F, which is translation invariant [30]. Formally, some features of the FPT properties of MA processes with a general state space have already been addressed in the mathematical literature using algebraic methods (see, e.g. [31]). Yet, explicit results on the FPT statistics for MA processes are sparse. Moreover, the interplay between (non)recurrent motion and Markovian switching between internal states and its comparison to standard Markov diffusion processes remains elusive.

[4] With a logarithmic correction in dimension 2.

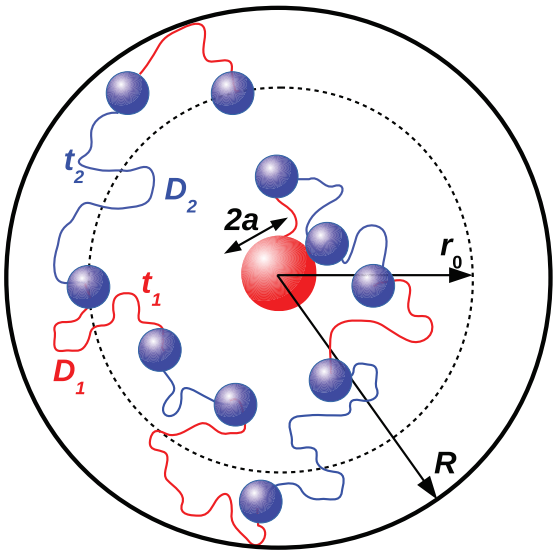

Figure 1. Schematic of the model system: a particle performs $3d$ Brownian motion in a spherical domain with a reflecting confining boundary at R and randomly switches between diffusion coefficients D_1 and D_2. The duration of the respective phases is exponentially distributed with rates $k_{1,2}$. The particle only recognises the target (red sphere in the centre) in phase 1—the recognition mode, whereas it experiences the target as a reflecting sphere in phase 2—the non-recognition mode.

Here we present rigorous results for the MFPT and FPT statistics for two-channel Markov additive diffusion[5] in a 3-dimensional spherical domain with the additive component F being Markovian. We consider a gated particle, that is, the particle can only recognise the target in one of the modes, which is shown to lead to non-trivial FPT behaviour. We also address the FPT problem of transitioning to an immobile phase. In particular, we prove that despite the perfectly non-recurrent motion of two-channel Markov additive diffusion in 3 dimensions, the MFPT does not fully specify the asymptotic exponential decay of the FPT statistics as soon as none of the phases is static (i.e. has a vanishing diffusion coefficient), in contrast to the standard Markovian counterpart.

The paper is organised as follows. First we set up the model of two-channel MA as a mixed boundary value problem for two coupled forward Fokker–Planck equations. Next, we summarise our main results on the MFPT and FPT statistics and discuss the implications of our results in a biophysical context. In the following sections we present detailed calculations, proofs and additional technicalities. As these contain essential mathematical approaches we include here all crucial steps of the derivation. Finally, we give a concluding perspective and discuss possible extensions of the work.

2. Markov additive two-channel diffusion

We consider a 3-dimensional spherical domain of size R with a perfectly absorbing target with radius a at the centre (see figure 1). The particle's diffusion coefficient D_k, i.e. the internal variable, randomly switches between states $k = 1$ and $k = 2$ in a Markovian fashion with rates

[5] Note that the term 'double diffusion' also appears in the literature [32].

k_1 and k_2, respectively. In other words, the duration of the respective phases is exponentially distributed with mean $\langle\tau_1\rangle = k_1^{-1}$ and $\langle\tau_2\rangle = k_2^{-1}$. At any instance, the particle's dynamics on infinitesimal time-scales Δt can be discretized as (see e.g. [7, 33])

$$\mathbf{x}_i(t+\Delta t) = \begin{cases} \mathbf{x}_j(t) & \text{w.p.} \quad k_i\Delta t, \\ \mathbf{x}_i(t) + \sqrt{2D_i\Delta t}\,\boldsymbol{\xi}(t) & \text{w.p.} \quad 1 - k_i\Delta t. \end{cases} \tag{1}$$

Here w.p. denotes 'with probability' and with $i \neq j = 1, 2$ and ξ_k being the component of a zero mean Gaussian white noise with $\langle\xi_k(t)\xi_l(t')\rangle = \delta(t-t')\delta_{kl}$[6]. We introduce the propagator $p(\mathbf{x}, t; i|\mathbf{y}, t'; j)$—the transition probability density for the particle to be at $\mathbf{x}$ at time t in internal state i given that it was previously at $\mathbf{y}$ at time t' in the internal state j. To first order in τ during any infinitesimal interval $\tau = t - t'$ the propagator can be split into two steps, (i) switching from j to the internal state i without diffusion, and (ii) diffusion in this new state without switching:

$$\begin{aligned} p(\mathbf{x}, t; i|\mathbf{y}, t'; j) &= \left[k_j\tau(1-\delta_{ij}) + \delta_{ij}(1-k_j\tau)(1+D_j\nabla^2)\right]\delta(\mathbf{x}-\mathbf{y}) \\ &= \left[(1-k_j\tau)\delta_{ij} + (k_j(1-\delta_{ij}) + \delta_{ij}\,D_j\nabla^2)\tau\right]\delta(\mathbf{x}-\mathbf{y}) + \mathcal{O}(\tau^2), \end{aligned} \tag{2}$$

where ∇^2 is taken with respect to $\mathbf{x}$. Using equation (2) as well as the Chapman-Kolmogorov equation [7, 33]

$$p(\mathbf{x}, t+\tau; i|\mathbf{y}, t'; j) = \int_\Omega \mathrm{d}\mathbf{z} \sum_{k=1}^{2} p(\mathbf{x}, t+\tau; i|\mathbf{z}, t; k)p(\mathbf{z}, t; k|\mathbf{y}, t'; j), \tag{3}$$

we obtain, upon taking the limit $\tau \to 0$ the forward Fokker–Planck equation (FPE), which for convenience we write in a vector form as

$$\partial_t \mathbf{p}^{\mathrm{T}}(\mathbf{x}, t|\mathbf{y}, t') = \begin{pmatrix} D_1\nabla^2 - k_1 & k_2 \\ k1 & D_2\nabla^2 - k_2 \end{pmatrix} \mathbf{p}^{\mathrm{T}}(\mathbf{x}, t|\mathbf{y}, t'), \tag{4}$$

where $\mathbf{p} = (p_1, p_2)$ is the transition probability density vector with the general initial condition $\mathbf{p}(\mathbf{x}, 0) = (w\delta(\mathbf{x}-\mathbf{x}_{0,1}), [1-w]\delta(\mathbf{x}-\mathbf{x}_{0,2}))$ with arbitrary real $w \in [0, 1]$. As the system is linear the solution to this general initial condition can be reconstructed from the solutions for $w = 1{,}0$ and $\mathbf{x}_{0,1} = \mathbf{x}_{0,2} = \mathbf{x}_0$. The FPE (4) is complemented by inhomogeneous boundary conditions at the surface of the target and confining boundary, $\partial\,\Omega_a$ and $\partial\,\Omega_R$, respectively:

$$\begin{aligned} &p_1(\mathbf{x}, t) = \left[\nabla p_2(\mathbf{x}, t)\right] \cdot \hat{\mathbf{n}}_a\Big|_{\mathbf{x}=\partial\Omega_a} = 0, \\ &\left[\nabla p_1(\mathbf{x}, t)\right] \cdot \hat{\mathbf{n}}_R = \left[\nabla p_2(\mathbf{x}, t)\right] \cdot \hat{\mathbf{n}}_R\Big|_{\mathbf{x}=\partial\Omega_R} = 0, \end{aligned} \tag{5}$$

where $\hat{\mathbf{n}}_a$ and $\hat{\mathbf{n}}_R$ denote the respective surface normals. The FPT probability density is obtained from the flux into the absorbing target from the recognition phase 1

$$\wp(t) = 4\pi a^2 D_1 \left[\nabla p_1(\mathbf{x}, t)\right] \cdot \hat{\mathbf{n}}_a\Big|_{\mathbf{x}=\partial\Omega_a} \tag{6}$$

and the MFPT corresponds to the first moment of $\wp(t)$, namely $\langle t\rangle = \int_0^\infty t\wp(t)\mathrm{d}t$. All quantities are made dimensionless by expressing time in units of $\tau_0 = R^2/D_1$, length, or in fact radii, in units of the domain radius $r_i \to x_i \equiv r_i/R$ and by introducing the dimensionless ratios $z = k_2/k_1$ and $\varphi = D_2/D_1$. Note that the time unit τ_0 is 'natural' as it holds trivially for any normal

[6] Here $\delta(x)$ and δ_{ik} denote the Dirac and Kroenecker delta functions, respectively.

diffusion process with a hyperspherical symmetry that the mean first passage time scales as $\langle t\rangle \propto R^2$ with the confining hypersphere radius R, irrespective of the dimension [32].

In the Brownian dynamics simulations reported herein the dynamics are implemented by first drawing a sojourn time τ_s from the respective exponential density with mean $k_{1,2}^{-1}$ and then propagating the particle's position within the interval τ_s according to the overdamped Langevin equation with the respective diffusion coefficient $D_{1,2}$. The initial condition is sampled uniformly over the surface of a sphere with radius r_0. Reflecting boundary conditions are implemented by neglecting any move that would take the particle into the reflecting boundary (while still updating the time). The particle is propagated until it reaches the target while being in the recognition mode 1.

3. Summary and discussion of the main results

3.1. Mean first passage times

We first focus on the MFPT. The proofs of the equations presented in this sections will be described in later sections. The MFPT to arrive at x_a if starting from x_0 in the recognition mode 1, $\langle t_{x_a}(x_0)\rangle_1$, is given exactly as

$$\langle t_{x_a}(x_0)\rangle_1 = \frac{1+z}{z+\varphi}\left[\langle t_{x_a}(x_0)\rangle_0 + \frac{\varphi(1-x_a^3)}{3z\overline{\mathcal{D}}_1(x_a)}\left(\frac{\overline{\Delta}_1(x_a)}{x_a} - \frac{\overline{\Delta}_1(x_0)}{x_0}\right)\right], \tag{7}$$

where we introduced the mean first passage time of standard 3-dimensional Brownian motion

$$\langle t_{x_a}(x_0)\rangle_0 = \frac{1}{3}\left(x_a^{-1} - x_0^{-1} - \frac{x_0^2 - x_a^2}{2}\right) \tag{8}$$

as well as the auxiliary functions

$$\begin{aligned}\overline{\mathcal{D}}_1(y) = {} & (1-y)\cosh[\sqrt{1+z/\varphi}\,(1-y)] \\ & + \frac{[y(1+z/\varphi)-1]\sinh[\sqrt{1+z/\varphi}\,(1-y)]}{\sqrt{1+z/\varphi}}\end{aligned} \tag{9}$$

$$\overline{\Delta}_1(y) = \cosh[\sqrt{1+z/\varphi}\,(1-y)] - \frac{\sinh[\sqrt{1+z/\varphi}\,(1-y)]}{\sqrt{1+z/\varphi}}. \tag{10}$$

Note that the prefactor in equation (7) is just the inverse of the effective diffusion coefficient $D_{\mathrm{eff}} = (D_1/k_1 + D_2/k_2)/(k_1^{-1} + k_2^{-1})$ expressed in units of D_1. Note that if the switching between the internal states is fast compared to the time needed to arrive to the vicinity of the target, then trajectories essentially behave as 3-dimensional Brownian motion with an effective diffusion coefficient D_{eff}. Thus $\langle t_{x_a}(x_0)\rangle_1$ has the form of the MFPT of standard 3-dimensional Brownian motion with D_{eff} plus a term compensating for the contribution of trajectories where the particle does not switch between modes sufficiently many times.

The result in equation (7) as a function of z for various values of k_1 and φ, divided by $\langle t_{x_a}(x_0)\rangle_0$, is depicted in figure 2(a) (full lines) and shows excellent agreement with Brownian dynamics simulations (symbols). Note that intuitively for sufficiently large $\varphi = D_2/D_1$, the MFPT $\langle t_{x_a}(x_0)\rangle_1$ can be significantly shorter than $\langle t_{x_a}(x_0)\rangle_0$. In addition, for sufficiently large k_1 there exists an optimal value of z where $\langle t_{x_a}(x_0)\rangle_1$ has a minimum. The optimisation of $\langle t_{x_a}(x_0)\rangle_1$,

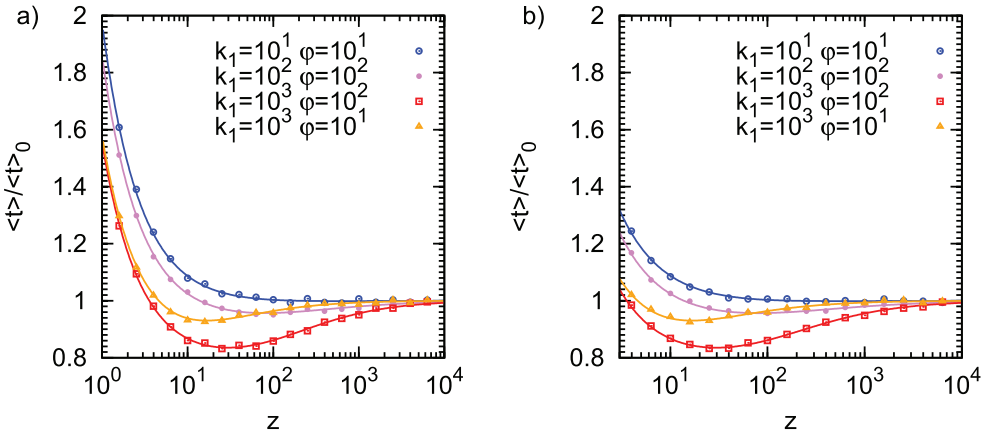

Figure 2. Normalised MFPT as a function of $z = k_2/k_1$ for various values of k_1 and φ. The results correspond to $x_0 = 0.5$ and $x_a = 0.01$. Panel (a) corresponds to a particle starting in the recognition mode 1, whereas (b) depicts the results for starting in the non-recognition mode 2.

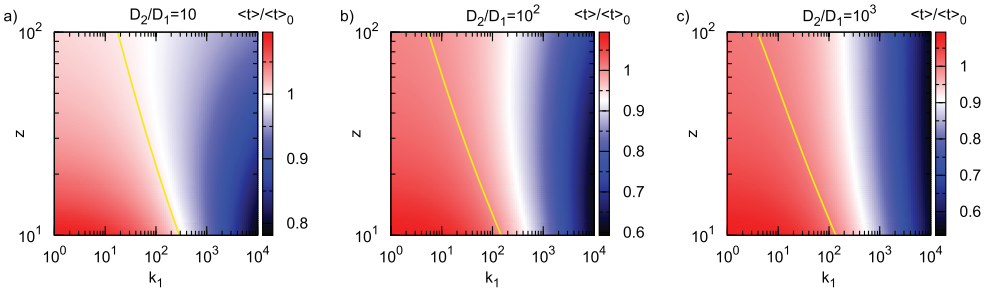

Figure 3. Normalised MFPT $\langle t_{x_a}(x_0)\rangle_1/\langle t_{x_a}(x_0)\rangle_0$ as a function of k_1 and $z = k_2/k_1$ for various φ and $x_0 = 0.5$ and $x_a = 0.01$. The yellow contour corresponds to $\langle t_{x_a}(x_0)\rangle_1/\langle t_{x_a}(x_0)\rangle_0 = 1$.

which essentially corresponds to solving a non-linear algebraic equation for z, is beyond the scope of the present work.

Additional insight is obtained from the joint dependence of $\langle t_{x_a}(x_0)\rangle_1$ on z and k_1. The results for three different values of φ are shown in figure 3. As already mentioned, for sufficiently large φ we find that $\langle t_{x_a}(x_0)\rangle_1$ intuitively decays with increasing k_1, as it is beneficial if the particle spends more time in the faster diffusing phase. The dependence on z is however, non-monotonic due to the simple fact that there is always a trade-off between reaching the target in the (faster) non-recognition mode and hitting the target from close distance through the recognition mode. For example, for large φ, the effective D_{eff} can become very large and consequently the MFPT can decrease substantially as long as z is not too close to φ, i.e. the particle spends enough time in the non-recognition mode. Intuitively, for $z \to \infty$ and φ finite D_{eff} converges to 1. However, if $z \to 0$, i.e. very long residence time in the non-recognition mode, the second term of equation (7) diverges as $1/z$ because even if the motion in mode 2 is fast enough to essentially reach a local steady state, the rate to switch back to the recognition mode becomes rate limiting.

Conversely, $\langle t_{x_a}(x_0)\rangle_2$, the MFPT to x_a starting from x_0 in the non-recognition mode 2 is given exactly as

$$\langle t_{x_a}(x_0)\rangle_2 = t^h_{\rm eff} + \frac{1+z}{z+\varphi}\left[\langle t_{x_a}(x_0)\rangle_0 + \frac{(1-x_a^3)}{3\overline{\mathcal{D}}_1(x_a)}\left(\frac{\varphi}{z}\frac{\overline{\Delta}_1(x_a)}{x_a} + \frac{\overline{\Delta}_1(x_0)}{x_0}\right)\right], \quad (11)$$

where we introduced the effective time to hit the target from the non-recognition mode 2 once arriving within a distance to the target, which corresponds to the typical distance moved in a switching cycle $k_1^{-1}+k_2^{-1}$

$$t^h_{\rm eff} = k_1^{-1}\frac{(D_1-D_2)/k_2}{D_1/k_1+D_2/k_2} \equiv k_1^{-1}\frac{1-\varphi}{z+\varphi}. \quad (12)$$

Note that the effective hitting-time correction $t^h_{\rm eff}$ can be positive or negative depending on φ. The result in equation (11) as a function of z for various values of k_1 and φ, expressed relative to $\langle t_{x_a}(x_0)\rangle_0$, is depicted in figure 2(b) (full lines) and as before shows excellent agreement with Brownian dynamics simulations (symbols). The joint dependence of $\langle t_{x_a}(x_0)\rangle_2$ on both z and k_1 for various φ is shown in figure 4. Qualitatively, the scenario of starting in the non-recognition mode is very similar to the previous one.

To understand the subtle difference between the two initial conditions more deeply we inspect the meaning of the effective hitting-time correction $t^h_{\rm eff}$ in equation (12) in more detail. If $\varphi \ll 1$ then $t^h_{\rm eff} \sim 1/k_2$, i.e. the correction time is equal to the mean time spent in the non-recognition mode. Conversely, $t^h_{\rm eff}$ gives a large negative contribution to $\langle t_{x_a}(x_0)\rangle_2$ when k_1 is small and $\varphi \gg 1$ and $\varphi \gg z$, that is, the particle resides over long periods in the recognition mode while simultaneously the typical distance moved in mode 2 is much larger than the one moved in mode 1, $D_2/k_2 \gg D_1/k_1$. The particle therefore has no difficulty in hitting the target from mode 2 as soon as it arrives to within a typical distance to it. However, as this also implies a small D_1 the natural time unit $\tau_0 = R^2/D_1$ explodes and the search time increases.

Finally, we inspect the scenario of intermittent immobilisation such as occurring in chromatography, i.e. $\varphi = 0$. We find from equations (7) and (11) that

$$\begin{aligned}\langle t_{x_a}(x_0)\rangle_{1,s} &= (1+z^{-1})\langle t_{x_a}(x_0)\rangle_0,\\ \langle t_{x_a}(x_0)\rangle_{2,s} &= (1+z^{-1})\langle t_{x_a}(x_0)\rangle_0 + k_2^{-1}.\end{aligned} \quad (13)$$

Note that the prefactor $1+z^{-1}$ is the inverse of the steady-state probability to be in the recognition mode 1. The results in equation (13) are intuitive as the diffusion coefficient becomes trivially reduced by the fraction of time spent in mode 1 (since mode 2 is static). Moreover, $\langle t_{x_a}(x_0)\rangle_{2,s}$ contains the additional term accounting for the fact that the particle needs to switch to mode 1 exactly once more since it starts from mode 2.

3.2. Probability density of first passage times

Due to the complexity of the problem it is not possible to obtain a general exact closed-form expression for $\wp(t)$ valid on all time scales. Therefore we here limit the discussion to the exact long time asymptotic of $\wp(t)$. In this section we simply state the results, whereas the proofs are presented in the next section. As intuitively expected (and proven in section 4.3) all moments of $\wp(t)$ are finite as long as $x_a > 0$ and $R < \infty$. Moreover, as $\wp(t)$ is smooth, this implies that it decays exponentially for long times, $\wp(t) \sim \mathcal{C}(x_0,x_a)\mathrm{e}^{-\lambda_0 t}$, where $\sim$ stands for asymptotic equality. Exact expressions for λ_0 and $\mathcal{C}(x_0,x_a)$ can be obtained from $\tilde{\wp}(s)$, the Laplace transform of the FPT density $\wp(t) = \hat{\mathcal{L}}^{-1}\{\tilde{\wp}(s)\}$. The results read

$$\lambda_0(x_a) = \sum_{k=1}^{\infty} \frac{v^{(0)}(x_a)^k}{v^{(1)}(x_a)^{2k-1}} \frac{\det \mathcal{M}_k}{(k-1)!} \tag{14}$$

$$\mathcal{C}(x_0, x_a) = \lim_{k\to\infty} \frac{\sum_{l=0}^{k-1} [u^{(l)}(x_0) - v^{(l)}(x_a)u^{(k)}(x_0)/v^{(k)}(x_a)]\,(-\lambda_0)^l/l!}{\sum_{l=0}^{k-1}\sum_{m=1}^{k-l} v^{(l+m)}(x_a)(-\lambda_0)^{l+m-1}/(l+m)!}, \tag{15}$$

where $u^{(k)}(x_0)$ and $v^{(k)}(x_a)$ denote the kth order derivative of the numerator and denominator of $\tilde{\wp}(s)$ with respect to s, respectively, evaluated at $s = 0$ as a function of x_a and x_0 (defined in section 4.3) and $\mathcal{M}_k$ stands for the 'almost' triangular matrix with elements

$$\begin{aligned}\mathcal{M}_k(i,j) = &\frac{v^{(i-j+2)}\Theta(i-j+1)}{(i-j+2)\,!} \\ &\times [k(i-j+1)\Theta(j-2) + i\Theta(1-j) + j - 1]\,,\end{aligned} \tag{16}$$

where $\Theta(n)$ denotes the discrete Heaviside step function and with the symbolic convention $\det\mathcal{M}_1 \equiv 1$. Note that equations (14) and (16) are fully general and are derived under very mild assumptions, which are warranted by the physics of the problem. More precisely, one has to assume (i) that all moments of $\wp(t)$ exist, (ii) that $\tilde{\wp}(s)$ has no branch points on the negative real axis, and (iii) that $\lim_{k\to\infty} u^{(k)}/v^{(k)} < \infty$. While (i) is satisfied trivially, (ii)[7] and (iii) are borne out in practice (see section 4.3).

We are particularly interested in the physically relevant scenario of a small target size. In the present case equation (14) actually defines a power series in x_a and we find in the limit $x_a \ll 1$ (note that for convenience we here present the inverse of λ_0)

$$\lambda_0^{-1}(x_a) = \langle t_{x_a}(1)\rangle_2 - \left[\frac{1+z}{z+\varphi}\right]\frac{1}{3\overline{\mathcal{D}}_1(x_a)} + \left[\frac{z/\varphi+\varphi}{z+\varphi}\right]\frac{\overline{\mathcal{D}'}_1(x_a)}{\overline{\mathcal{D}}_1(x_a)} + \mathcal{O}(x_a), \tag{17}$$

where we introduced the auxiliary function

$$\begin{aligned}\overline{\mathcal{D}'}_1(y) = &\frac{(1-y)[(1+z/\varphi)y - 1]\cosh[\sqrt{1+z/\varphi}\,(1-y)]}{(1+z/\varphi)} \\ &+\frac{[(1+z/\varphi)(1-y+y^2)+1]\sinh[\sqrt{1+z/\varphi}\,(1-y)]}{(1+z/\varphi)^{3/2}}.\end{aligned} \tag{18}$$

Analogously, the series in (15) converges with the first term for $x_a \to 0$ and we obtain the exact asymptotic result

$$\wp_{1,2}(t) \sim \langle t_{x_a}(x_0)\rangle_{1,2}\lambda_0^2(x_a)\mathrm{e}^{-\lambda_0(x_a)t}. \tag{19}$$

Equation (19) is the central result of this paper. It reveals that the exponential decay rate is independent of the initial condition (i.e. the position as well as the internal state). This regime describes indirect trajectories, which interact with the confining boundary before heading towards the target [10]. The fact that the decay rate of $\wp_{1,2}(t)$ is independent of the initial condition suggests that reaching the external boundary from the initial location is much faster than reaching the target from the external boundary. Moreover, only the prefactor depends on the initial condition—the position as well as internal state, which suggests the statistics of direct trajectories, i.e. those that reach the target without ever interacting with the boundary,

[7] One can show for most Markov processes, incl. Brownian motion (BM) in dimensions 1, 2, and 3, diffusion on fractals, uniformly biased 1-dimensional BM, radially biased 2-dimensional BM and the Ornstein-Uhlenbeck process, that $\tilde{\wp}(s)$ has only simple poles and removable singularities on the negative real axis [34].

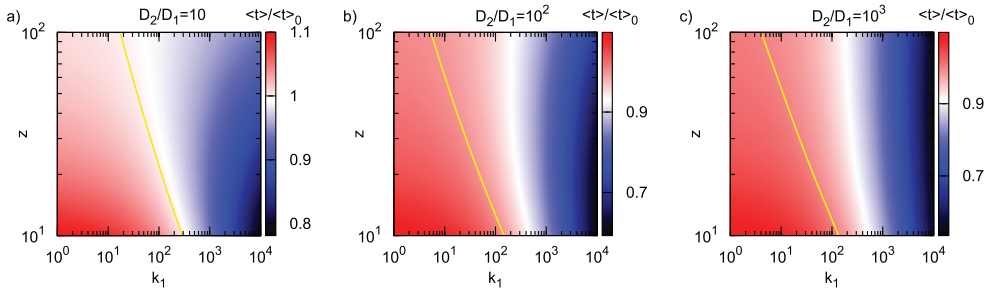

Figure 4. Normalised MFPT $\langle t_{x_a}(x_0)\rangle_2/\langle t_{x_a}(x_0)\rangle_0$ as a function of k_1 and $z = k_2/k_1$ for various φ and $x_0 = 0.5$ and $x_a = 0.01$. The yellow contour corresponds to $\langle t_{x_a}(x_0)\rangle_0/\langle t_{x_a}(x_0)\rangle_2 = 1$.

controls the statistical weight of the exponential asymptotic, which is equivalent to the simpler Markovian counterparts [10]. To see this we can rewrite equation (19) as a product of the 'weight' factor $\langle t_{x_a}(x_0)\rangle_{1,2}\lambda_0(x_a)$ and a normalised exponential $\mathrm{e}^{-\lambda_0(x_a)t}\lambda_0(x_a)$. Therefore, the contribution of the long-time regime to expectations taken over $\wp_{1,2}(t)$ will depend only on the 'weight' factor and the smallest time where equation (19) becomes valid.

Moreover, equation (19) highlights that the asymptotic of $\wp(t)$ *cannot* be fully reconstructed by knowing the MFPT, as both the prefactor and the exponent contain a non-trivial correction term in λ_0. This observation is in stark contrast to the simpler Markovian counterpart, where the $\wp(t)$ asymptotic can indeed be reconstructed once the MFPT is known (see [10, 19]) as long as the dynamics is non-recurrent, highlighting the non-trivial first passage character of Markov additive processes.

Furthermore, if we rescale time according to $\theta \equiv t/\lambda_0(x_a)$, then all FPT densities must collapse onto the master curve

$$\overline{\wp}_{1,2}(\theta) \equiv \wp_{1,2}(\theta)/[\lambda_0^2(x_a)\langle t_{x_a}(x_0)\rangle_{1,2}] = \mathrm{e}^{-\theta}. \tag{20}$$

Indeed, this collapse is shown in figure 5 for a variety of parameters and initial conditions.

In the case of a static non-recognition mode we again find for $x_a \ll 1$ an intuitive renormalisation of the diffusion coefficient and we can identify the universal form for non-recurrent single-channel Markov dynamics [10]

$$\wp^s_{1,2}(t) \sim \langle t_{x_a}(x_0)\rangle_{1,2;s}\langle t_{x_a}(1)\rangle^{-2}_{2,s}\mathrm{e}^{-t/\langle t_{x_a}(1)\rangle_{2,s}}. \tag{21}$$

Note that in contrast to $\varphi \neq 0$ (see equation (19)), the transient immobilisation case leads to a Poisson-like asymptotic (21) [10, 19].

3.3. Biophysical implications of the results

The stochastic switching between different internal states is relevant in various biophysical problems, in particular in cellular signalling pathways. Namely, proteins can switch between different conformations with different diffusivities, either spontaneously or upon interaction with other signalling molecules [4, 7, 29]. Similarly, in the regulation of gene transcription regulatory proteins can change the affinity of TF for the promoter site [35, 36]. Most proteins transiently bind non-specifically to other proteins and other cytoplasmic constituents, incl. immobilised structures [37, 38]. Furthermore, some signalling molecules such as calmodulin (a cellular calcium sensor) are intrinsically 'sticky' and bind to various cytoplasmic constituents when biochemically stimulated (in the case of calmodulin by calcium [38]), and as a

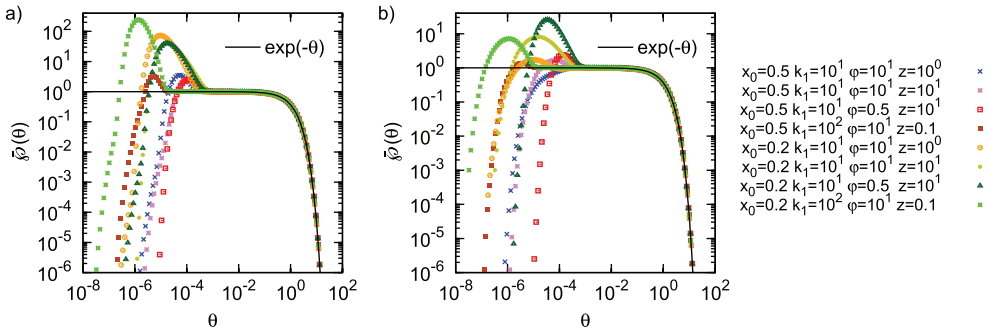

Figure 5. Rescaled FPT probability density $\overline{\wp}_{1,2}(\theta) \equiv \wp_{1,2}(\theta)/(\lambda_0^2(x_a)\langle t_{x_a}(x_0)\rangle_{1,2})$ obtained from Brownian dynamics simulations as a function of the rescaled time $\theta = t/\lambda_0$ for $x_a = 0.01$ and various k_1,z and φ and two different initial conditions x_0 for the scenario of (a) starting in the recognition mode and (b) starting in the non-recognition mode. The full black line corresponds to the unit exponential master scaling in equation (20). The simulation results perfectly collapse on the master curve.

result display a smaller diffusion coefficient in the activated mode. In these cases only the active form typically binds to its target and triggers a biological response. The cellular regulation machinery can adjust the binding rates and hence the resulting spatio-temporal dynamics of signalling molecules [4, 38].

Therefore, in biological systems wide ranges of z and φ occur and may have been selected by evolution. In the biophysical context the first passage time problem studied here would correspond to the association time of a signalling molecule with its target. Our results show that changing z and φ can profoundly affect the association dynamics. In particular, our results demonstrate that it is possible to tune specific stages of the target search process, such as delivery to the target from a distance or the hitting step from close proximity. Conversely, our findings highlight the fact that the dynamics cannot be quantified in terms of effective parameters alone, e.g. with an average diffusion coefficient. Nor can the first arrival time statistics be specified solely on the basis of MFPT concepts.

4. Proofs and details of calculations

In this section we describe details of the calculations and provide proofs of the equations presented in the previous section.

4.1. Solution of the coupled mixed boundary value problem

To solve equation (4) we first introduce auxiliary dimensionless coordinates $\mathbf{x}' = \sqrt{k_1/D_1}\,\mathbf{x}$ and $t' = k_1 t$ and Laplace transform in time $\tilde{\mathbf{p}}^{\mathrm{T}} = \hat{\mathcal{L}}[\mathbf{p}^{\mathrm{T}}; t' \to s]$. Defining for convenience $z = k_2/k_1$ and $\varphi = D_2/D_1$, we find that the components of $\tilde{\mathbf{p}}^{\mathrm{T}}$ obey

$$(\nabla^2 - 1 - s)\tilde{p}_1 + z\tilde{p}_2 = -\frac{w}{4\pi r_0'^2\sqrt{k_1 D_1}}\delta(r' - r_0') \tag{22}$$

$$(\varphi\nabla^2 - z - s)\tilde{p}_2 + \tilde{p}_1 = -\frac{(1-w)}{4\pi r_0'^2\sqrt{k_1 D_1}}\delta(r' - r_0'), \tag{23}$$

where we take either $w = 1$ or $w = 0$, as any other solution is obtained by linear superposition of these solutions. Since we assume that initially the particle's position is uniformly distributed over the surface of a sphere with radius r_0 (see section 2), the boundary value problem in equations (22) and (23) becomes effectively 1-dimensional in the radial coordinate. Equations (22) and (23) show that $\tilde{p}_{1,2}$ correspond to the Green's functions of our coupled mixed boundary value problem. The general solution to the homogeneous coupled equations is obtained by inserting equation (23) into equation (22) to obtain the 4th order PDE for $\tilde{p}_1$

$$\{\varphi\nabla^4 - [(\varphi+1)s + \varphi + z]\nabla^2 + s(s+z+1)\}\tilde{p}_1 = 0. \tag{24}$$

To solve it we make the standard ansatz

$$\nabla^2\tilde{p}_1 = q\tilde{p}_1 \tag{25}$$

such that q is the root of the quadratic equation

$$\varphi q^2 - [(\varphi+1)s + \varphi + z]q + s(s+z+1) = 0 \tag{26}$$

or explicitly,

$$q_\pm(s) = \frac{1}{2\varphi}\left[(\varphi+1)s + \varphi + z \pm \sqrt{[(1-\varphi)s + (z-\varphi)]^2 - 4\varphi z}\right]. \tag{27}$$

The general solution of equations (22) and (23) for a 3-dimensional system with spherical symmetry can now be written as

$$\tilde{p}_1(r',s) = r'^{-1}\left(C_1 e^{-\sqrt{q_+}r'} + C_2 e^{\sqrt{q_+}r'} + C_3 e^{-\sqrt{q_-}r'} + C_4 e^{\sqrt{q_-}r'}\right) \tag{28}$$

$$\begin{aligned}\tilde{p}_2(r',s) = \Bigg(&\frac{s+1-q_+}{r'z}\left[C_1 e^{-\sqrt{q_+}r'} + C_2 e^{\sqrt{q_+}r'}\right] \\ &+ \frac{s+1-q_-}{r'z}\left[C_3 e^{-\sqrt{q_-}r'} + C_4 e^{\sqrt{q_-}r'}\right]\Bigg),\end{aligned} \tag{29}$$

where equation (28) is obtained as a solution of equations (25) and (29) is obtained by first inserting the solution (28) into the homogeneous form of equation (22) and then solving for $\tilde{p}_2$. Moreover, C_1 to C_4 are constants determined by the boundary conditions in equation (5), and the continuity and jump discontinuity of the Green's functions in equations (22) and (23). These lead to two inhomogeneous systems of 8 linear equations with 8 unknowns, C_1 to C_4 for $r \leqslant r_0$ and C_5 to C_8 for $r > r_0$, for each of the cases $w = 0$ and $w = 1$, respectively. These are in turn solved by Cramer's rule. We omit these calculations as they are tedious but straightforward.

The Laplace transformed FPT density $\tilde{\wp}(s)$ in the dimensionless units introduced in section 2 is obtained from the flux into the absorbing boundary (i.e. from the Laplace transform of equation (6)) and in the final form reads for the recognition and non-recognition initial condition, respectively,

$$\tilde{\wp}_1(s) = \left(\frac{x_a}{x_0}\right)\frac{Q_2(s)\Delta_1(s,x_0)\mathcal{D}_2(s,x_a) - Q_1(s)\Delta_2(s,x_0)\mathcal{D}_1(s,x_a)}{Q_2(s)\Delta_1(s,x_a)\mathcal{D}_2(s,x_a) - Q_1(s)\Delta_2(s,x_a)\mathcal{D}_1(s,x_a)}, \tag{30}$$

$$\tilde{\wp}_2(s) = \left(\frac{x_a}{x_0}\right)\frac{\varphi^{-1}[\Delta_2(s,x_0)\mathcal{D}_1(s,x_a) - \Delta_1(s,x_0)\mathcal{D}_2(s,x_a)]}{Q_2(s)\Delta_1(s,x_a)\mathcal{D}_2(s,x_a) - Q_1(s)\Delta_2(s,x_a)\mathcal{D}_1(s,x_a)}. \tag{31}$$

Here we introduced the auxiliary functions $Q_{1,2}(s) = (s + k_1 - k_1 q_{+,-}(s))/(k_1 z)$ as well as

$$\mathcal{D}_{1,2}(s,y) = (1-y)\cosh[\sqrt{k_1 q_{+,-}(s)}\,(1-y)] + \frac{[\,y k_1 q_{+,-}(s) - 1]\sinh[\sqrt{k_1 q_{+,-}(s)}\,(1-y)]}{\sqrt{k_1 q_{+,-}(s)}} \tag{32}$$

$$\Delta_{1,2}(s,y) = \cosh[\sqrt{k_1 q_{+,-}(s)}\,(1-y)] - \frac{\sinh[\sqrt{k_1 q_{+,-}(s)}\,(1-y)]}{\sqrt{k_1 q_{+,-}(s)}}, \tag{33}$$

where we always take the first or second index on both sides, respectively. Note that here we already back-transformed the auxiliary coordinates $\mathbf{x}' \to \mathbf{x}$ and $s \to s/k_1$. Obviously, $\overline{\mathcal{D}}_1(y) = \mathcal{D}_1(0,y)$ and $\overline{\Delta}_1(y) = \Delta_1(0,y)$ (see equations (9) and (10)). Note that $\tilde{\wp}_{1,2}(s)$ has a removable singularity at $s = 0$, therefore we re-define the analytic function $\tilde{\wp}_{1,2}(s)$ at $s = 0$ as $\tilde{\wp}_{1,2}(0) \equiv \lim_{s\to 0} \tilde{\wp}_{1,2}(s)$.

4.2. Mean first passage times

Proving equations (7) and (11) is henceforth easy, and is carried out by taking the derivative of equations (30) and (31)

$$\langle t_{x_a}(x_0)\rangle_{1,2} = -\left.\frac{\partial \tilde{\wp}_{1,2}(s)}{\partial s}\right|_{s=0}. \tag{34}$$

Noticing that $\overline{\mathcal{D}}_2(y) = 0$, $\overline{\Delta}_2(y) = y$ as well as $q_-(0) = 0$, $q_+(0) = k_1(1 + z/\varphi)$, and finally $q'_+(0) = (z/\varphi + \varphi)/(z + \varphi)$, $q'_-(0) = (1 + z)/(z + \varphi)$, and performing some elementary algebraic manipulations already completes the proof of equations (7) and (11). □

4.3. Inverse Laplace transform of $\tilde{\wp}(s)$

4.3.1. Justification of assumptions (i)–(iii) made in section 3.2. Note that the analytic function $\tilde{\wp}(s)$ defined in section 4.1 is regular at $s = 0$, has no branch points on the negative real axis (hence justifying assumption (ii) in section 3.2) and allows a moment expansion $\tilde{\wp}(s) = \sum_{n=0}^{\infty}(-s)^n\langle t^n\rangle/n!$ converging for $\mathrm{Re}(s) < \lambda_0$, where $-\lambda_0 \in \mathbb{R}$ is the pole of $\tilde{\wp}(s)$ closest to the origin [34]. This also implies that all moments of $\wp(t)$ are finite, which justifies assumption (i) in section 3.2 [34]. Moreover, the moments $\langle t^n\rangle$ are obtained recursively from Taylor coefficients of the series of the numerator and denominator of equations (30) and (31), $\sum_{k=0}^{\infty} u_{1,2}^{(k)}(0)s^k/k!$ and $\sum_{k=0}^{\infty} v^{(k)}(0)s^k/k!$, respectively,

$$\langle t^n\rangle = (-1)^n\frac{u^{(n)}(0)}{v^{(0)}(0)} - \sum_{k=1}^{n}(-1)^k\binom{n}{k}\frac{v^{(k)}(0)}{v^{(0)}(0)}\langle t^{n-k}\rangle. \tag{35}$$

Explicitly, the coefficients $u_1^{(k)}(0)$ of the numerator read

$$
\begin{aligned}
u_1^{(n)}(0) = n\,! \left(\frac{1+\varphi}{k_1(z+\varphi)}\right)^n \sum_{k=0}^{\infty}\left(\frac{k_1(z+\varphi)}{2\varphi}\right)^k \\
\times \sum_{l=0}^{k} \frac{(1-x_0)^{2(k-l)}(1-x_a)^{2l+1}[2(k-l)+x_a]}{(2[k-l]+1)\,!\,(2l+1)\,!} \\
\times \left[\mathcal{S}_1(k,l,n) + \mathcal{S}_2(k,l,n) + \mathcal{S}_3(k,l,n) + \mathcal{S}_4(k,l,n) - \mathcal{S}_5(k,l,n)\right]
\end{aligned} \tag{36}
$$

where the functions $\mathcal{S}_1$ to $\mathcal{S}_5$ are defined as

$$
\begin{aligned}
\mathcal{S}_1(k,l,n) = \frac{2l(1-x_a)-x_a}{x_0 z} \sum_{i=0}^{\lfloor\frac{k-l}{2}\rfloor\wedge\lfloor\frac{l}{2}\rfloor} \Theta(k-n) \\
\times\Theta(k-2\mathrm{i}-n)\Theta(2\mathrm{i}-n)W_{k-l,l,i}\Xi_{n,k-l,l,i},
\end{aligned} \tag{37}
$$

$$
\begin{aligned}
\mathcal{S}_2(k,l,n) = \frac{2l(1-x_a)+x_a(k_1-1)}{x_0 k_1 z} \sum_{i=0}^{\lfloor\frac{k-l}{2}\rfloor\wedge\lfloor\frac{l+1}{2}\rfloor} \Theta(k+1-n) \\
\times\Theta(k+1-2\mathrm{i}-n)\Theta(2\mathrm{i}-n)W_{k-l,l+1,i}\Xi_{n,k-l,l+1,i},
\end{aligned} \tag{38}
$$

$$
\begin{aligned}
\mathcal{S}_3(k,l,n) = \frac{2l(1-x_a)-x_a}{x_0 k_1 z} \sum_{i=0}^{\lfloor\frac{k-l}{2}\rfloor\wedge\lfloor\frac{l}{2}\rfloor} \Theta(k+1-n) \\
\times\Theta(k+1-2\mathrm{i}-n)\Theta(2\mathrm{i}+1-n)W_{k-l,l,i}\Xi_{n-1,k-l,l,i},
\end{aligned} \tag{39}
$$

$$
\begin{aligned}
\mathcal{S}_4(k,l,n) = \frac{x_a}{x_0 k_1 z} \sum_{i=0}^{\lfloor\frac{k-l}{2}\rfloor\wedge\lfloor\frac{l+1}{2}\rfloor} \Theta(k+2-n) \\
\times\Theta(k+2-2\mathrm{i}-n)\Theta(2\mathrm{i}+1-n)W_{k-l,l+1,i}\Xi_{n-1,k-l,l+1,i},
\end{aligned} \tag{40}
$$

$$
\begin{aligned}
\mathcal{S}_5(k,l,n) = \frac{x_a}{x_0 k_1 z} \sum_{i=0}^{\lfloor\frac{k-l}{2}\rfloor\wedge\lfloor\frac{l+2}{2}\rfloor} \Theta(k+2-n) \\
\times\Theta(k+2-2\mathrm{i}-n)\Theta(2\mathrm{i}-n)W_{k-l,l+2,i}\Xi_{n,k-l,l+2,i},
\end{aligned} \tag{41}
$$

where $\Theta(n)$ is the discrete Heaviside step function, $\lfloor x\rfloor$ is the floor function, $x\wedge y\equiv\min(x,y)$ and

$$
\begin{aligned}
W_{p,q,i} = \sum_{j=0}^{i} \Bigg\{\Theta(\lfloor q/2-1\rfloor - j)\Theta(\lfloor p/2\rfloor - i)\binom{p}{2\mathrm{i}}\binom{q}{2j+1} \\
+ \Theta(\lfloor q/2\rfloor - j)\Theta(\lfloor p/2-1\rfloor - i)\binom{p}{2j+1}\binom{q}{2\mathrm{i}}\Bigg\},
\end{aligned} \tag{42}
$$

and where we also introduced

$$
\begin{aligned}
\Xi_{k,p,q,i} = \sum_{m=0}^{k} \Theta(p+q-2\mathrm{i}+m-k)\Theta(2\mathrm{i}-m)\binom{p+q-2\mathrm{i}}{k-m}\binom{2\mathrm{i}}{m} \\
\times\left[\frac{(1-\varphi)(z+\varphi)}{(1+\varphi)(z-\varphi)}\right]^m \left[\frac{(z-\varphi)^2}{k_1 z\varphi}\right]^{\lfloor(k-m)/2\rfloor}\binom{2\mathrm{i}}{\lfloor(k-m)/2\rfloor} \\
\times {}_2F_1\left\{1, \lfloor(k-m)/2\rfloor - 2\mathrm{i}, 1+\lfloor(k-m)/2\rfloor; -\frac{(z-\varphi)^2}{k_1 z\varphi}\right\}.
\end{aligned} \tag{43}
$$

Finally, ${}_2F_1\{i,j,k;z\}$ denotes the Gauss hypergeometric function. The coefficients $v^{(k)}(0)$ of the denominator are obtained by replacing x_0 with x_a.

For the scenario of starting in the non-recognition mode the Taylor series of the numerator is simpler and the coefficients read

$$\begin{aligned} u_2^{(n)}(0) = -\frac{n!}{\varphi}\left(\frac{1+\varphi}{k_1(z+\varphi)}\right)^n \sum_{k=0}^{\infty}\left(\frac{k_1(z+\varphi)}{2\varphi}\right)^k \\ \times \sum_{l=0}^{k} \frac{(1-x_0)^{2(k-l)}(1-x_a)^{2l+1}[2(k-l)+x_a]}{(2[k-l]+1)!(2l+1)!} \\ \times[k_1 z\mathcal{S}_1(k,l,n) + \frac{x_a}{x_0}\Theta(k+1-n) \sum_{i=0}^{\lfloor\frac{k-l}{2}\rfloor\wedge\lfloor\frac{l+1}{2}\rfloor} \Theta(k+1-2\mathrm{i}-n) \\ \times\Theta(2\mathrm{i}-n)W_{k-l,l+1,i}\Xi_{n,k-l,l+1,i}\big]. \end{aligned} \tag{44}$$

The calculation leading to the Taylor series (36) and (44) is essentially straightforward and amounts to combining the respective Taylor series of the individual functions occurring in equations (30) and (31) and carefully performing a sequence of changes of the order of summations thereby bringing the summation over powers of s to the outermost sum. The numerous step functions $\Theta(x)$ in the expressions for the coefficients are merely a consequence of the preservation of the domain of summation upon changing the order in which they are carried out.

The coefficients $u_1^{(k)}(0)$, $u_2^{(k)}(0)$ and $v^{(k)}(0)$ are hence given in the form of convergent series and it is not difficult to check (e.g. using Mathematica) that $\lim_{n\to\infty} u_1^{(n)}(0)/v^{(n)}(0) = 0$ and $\lim_{n\to\infty} u_2^{(n)}(0)/v^{(n)}(0) = 0$, thereby justifying the assumption (iii) of section 3.2, that is $\lim_{n\to\infty} u^{(n)}(0)/v^{(n)}(0) < \infty$. Summing up this now justifies assumptions (i)–(iii) in section 3.2, i.e. the necessary conditions for the validity of equations (14)–(16) [34].

4.3.2. Asymptotic inversion of the Laplace transform. Since $\tilde{\wp}(s)$ has no branch points we can invert it using Cauchy's theorem

$$\wp(t) \sim \lim_{s\to-\lambda_0} [(s+\lambda_0)\tilde{\wp}(s)\mathrm{e}^{st}], \tag{45}$$

where the contour used to evaluate the residue is chosen as to enclose $-\lambda_0$ such that $\mathbb{R}(s) < \lambda_0$. A rigorous solution to this problem, i.e. determining λ_0 and evaluating the residue in equation (45), was obtained recently under the assumptions (i)–(iii) in section 3.2 [34]. A detailed proof is given in [34]. Here we merely state the result, which has the form of equations (14)–(16).

To proceed towards our central result equation (19) we note that the first terms of the series (14) are

$$\lambda_0(x_a) = \frac{v^{(0)}(x_a)}{v^{(1)}(x_a)}\left(1 + \frac{v^{(0)}(x_a)}{2}\frac{v^{(2)}(x_a)}{v^{(1)}(x_a)^2}[1+\mathcal{O}]\right), \tag{46}$$

where $\frac{v^{(0)}(x_a)}{2}\frac{v^{(2)}(x_a)}{v^{(1)}(x_a)^2}$ is of the order of x_a and moreover, $\mathcal{O}$ is also of the order of x_a. This can be seen either by computing the respective derivatives explicitly or from the Taylor coefficients in equation (36) by making the replacement $x_0 \to x_a$. Therefore all correction terms vanish in the limit $x_a \to 0$, and equations (14) and (15) both fully converge already with the first term, which completes the proof of equation (19). □

5. Conclusion

Our results highlight the complex character of the first passage time statistics of Markov additive processes. While it appears to be a common feature of non-recurrent Markov processes that the first passage time asymptotics can be fully reconstructed from the corresponding mean first passage time [10, 19], we here showed that this is not the case for Markov additive processes. The present results on a Markovian sum of two perfectly non-recurrent Bessel processes establish rigorously the non-trivial connection between mean first passage times and long time first passage asymptotics. In addition, we also obtained results for the case of transient immobilisation, i.e. the transitioning into an immobile phase.

The results of this paper are important in a broader context, as most existing studies of the first passage behaviour of Markov additive processes are limited to the analysis of mean first passage times [7, 21, 25]. Moreover, our results also demonstrate that the first passage behaviour of Markov additive processes in general cannot be adequately captured by effective quantities such as the effective diffusion coefficient. This is important if one would attempt to develop effective medium or averaging type approximations.

The exact Laplace inversion formula presented in this paper (equations (14)–(16)) will be useful in various problems, as it reduces the problem of deriving first passage asymptotics to the much simpler problem of finding the Laplace transform of the first passage time density. It will also be very useful for developing singular perturbation results, such as the small target limit studied here.

The present results can be extended in numerous ways. For instance, a straightforward extension would be to include more internal states, or to combine diffusive and advective states such as in the intermittent search model [21] or in the presence of so-called cytoplasmic streaming in cells [39]. One could also take into account the spatial heterogeneity of diffusion coefficients [9, 10, 40], spatial or energetic disorder [41] or consider a more complex fluctuating environment [42]. Similarly, one could address the role of anomalous diffusion, such as observed in the motion of proteins and submicron objects in the cell cytoplasm [43].

Acknowledgments

We thank A Cherstvy for stimulating discussions. AG acknowledges funding through an Alexander von Humboldt Fellowship and ARRS project Z1-7296.

References

[1] Redner S 2001 *A Guide to First Passage Processes* (New York: Cambridge University Press) (doi: 10.1017/CBO9780511606014)
[2] Metzler R, Oshanin G and Redner S (ed) 2014 *First-Passage Phenomena and Their Applications* (Singapore: World Scientific)
[3] von Smoluchowski M 1916 *Phys. Z.* **17** 557
[4] Alberts B *et al* 2002 *Molecular Biology of the Cell* (New York: Garland)
[5] Schuss Z, Singer A and Holcman D 2007 *Proc. Natl Acad. Sci. USA* **104** 16098
Rupprecht J F, Bénichou O, Grebenkov D S and Voituriez R 2015 *J. Stat. Phys.* **158** 192
Grebenkov D S and Oshanin G 2016 arXiv:1609.00948
[6] Holcman D and Schuss Z 2015 *Stochastic Narrow Escape in Molecular and Cellular Biology* (New York: Springer) (doi: 10.1007/978-1-4939-3103-3)
[7] Reingruber J and Holcman D 2009 *Phys. Rev. Lett.* **103** 148102
Reingruber J and Holcman D 2010 *J. Phys.: Condens. Matter* **22** 065103
[8] Pulkkinen O and Metzler R 2013 *Phys. Rev. Lett.* **110** 198101

[9] Godec A and Metzler R 2015 *Phys. Rev.* E **91** 052134
[10] Godec A and Metzler R 2016 *Sci. Rep.* **6** 20349
[11] Mejía-Monasterio C, Oshanin G and Schehr G 2011 *J. Stat. Mech.* P06022
Mattos T G, Mejía-Monasterio C, Metzler R and Oshanin G 2012 *Phys. Rev.* E **86** 031143
[12] ben-Avraham D and Havlin S 2002 *Diffusion and Reactions in Fractals and Disordered Systems* (Cambridge: Cambridge University Press) (doi: 10.1017/CBO9780511605826)
[13] Berkowitz B, Cortis A, Dentz M and Scher H 2006 *Rev. Geophys.* **44** RG2003
Scher H, Margolin G, Metzler R, Klafter J and Berkowitz B 2002 *Geophys. Res. Lett.* **29** 1061
[14] Berg H C 1993 *Random Walks in Biology* (Princeton, NJ: Princeton University Press)
Schwarzl M, Godec A, Oshanin G and Metzler R 2016 *J. Phys. A: Math. Theor.* **49** 225601
Oshanin G, Vasilyev O, Krapivsky P L and Klafter J 2009 *Proc. Natl Acad. Sci. USA* **106** 13696
Bell W J 1991 *Searching Behaviour* (London: Chapman & Hall) (doi: 10.1007/978-94-011-3098-1)
Palyulin V V, Chechkin A V and Metzler R 2014 *Proc. Natl Acad. Sci. USA* **111** 2931
[15] Lloyd A L and May R M 2001 *Science* **292** 1316–7
[16] Hufnagel L, Brockmann D and Geisel T 2004 *Proc. Natl Acad. Sci. USA* **101** 15124
[17] Mantegna R N and Stanley H E 2007 *Introduction to Econophysics: Correlations and Complexity in Finance* (Cambridge: Cambridge University Press)
[18] Bray A J, Majumdar S N and Schehr G 2013 *Adv. Phys.* **62** 325
[19] Bénichou O and Voituriez R 2014 *Phys. Rep.* **539** 225
[20] Oshanin G, Lindenberg K, Wio H S and Burlatsky S 2009 *J. Phys. A: Math. Theor.* **42** 434008
[21] Bénichou O, Loverdo C, Moreau M and Voituriez R 2011 *Rev. Mod. Phys.* **83** 81
Bénichou O, Loverdo C, Moreau M and Voituriez R 2008 *Nat. Phys.* **9** 134
Bénichou O, Loverdo C, Moreau M and Voituriez R 2009 *J. Stat. Mech.* P02045
[22] Godec A and Metzler R 2015 *Phys. Rev.* E **92** 010701
[23] Godec A and Metzler R 2016 *J. Phys. A: Math. Theor.* **49** 364001
[24] Lomholt M A, Koren T, Metzler R and Klafter J 2008 *Proc. Natl Acad. Sci. USA* **105** 11055
[25] Hippel P H and Berg O G 1989 *J. Biol. Chem.* **264** 675
Sheinman O, Bénichou O, Kafri Y and Voituriez R 2012 *Rep. Prog. Phys.* **75** 026601
Bauer M and Metzler R 2012 *Biophys. J.* **102** 2321
Bauer M and Metzler R 2013 *PLoS One* **8** e53956
Koslover E F, Díaz de la Rosa M A D and Spakowitz A J 2011 *Biophys. J.* **101** 856
Kolomeisky A 2011 *Phys. Chem. Chem. Phys.* **13** 2088
Wunderlich Z and Mirny L A 2008 *Nucl. Acids Res.* **36** 3570
[26] Lomholt M A, van den Broek B, Kalisch S-M J, Wuite G J L and Metzler R 2009 *Proc. Natl Acad. Sci. USA* **106** 8204
[27] Lomholt M A, Ambjörnsson T and Metzler R 2005 *Phys. Rev. Lett.* **95** 260603
[28] Slutsky M and Mirny L A 2004 *Biophys. J.* **87** 4021
Bauer M, Rasmussen E S, Lomholt M A and Metzler R 2015 *Sci. Rep.* **5** 10072
[29] Szabo A, Schulten K and Schulten Z 1980 *J. Chem. Phys.* **72** 4350
Szabo A, Shoup D, Northrup S and McCammon J 1982 *J. Chem. Phys.* **77** 4484
Zwanzig R 1992 *J. Chem. Phys.* **97** 3587
Berezhkovski A, Yang D, Sheu S and Lin S 1996 *Phys. Rev. E* **54** 4462
Makhnovski Y *et al* 1998 *J. Chem. Phys.* **108** 971
Doering C and Gadoua J 1992 *Phys. Rev. Lett.* **69** 2318
Bier M and Astumian R 1993 *Phys. Rev. Lett.* **71** 1649
Holcman D and Schuss Z 2005 *J. Chem. Phys.* **122** 114710
[30] Ney P and Nummelin E 1987 *Ann. Probab.* **15** 561
Ney P and Nummelin E 1987 *Ann. Probab.* 15 593 Arjas E and Speed T P 1973 *Math. Scand.* **33** 171
[31] D'Auria B, Ivanovs J, Kella O and Mandjes M 2010 *J. Appl. Probab.* **47** 1048
[32] Hughes B D 1995 *Random Walks and Random Environments, Volume 1: Random Walks* (Oxford: Clarendon)
[33] Schuss Z 2010 *Theory and Applications of Stochastic Processes: an Analytical Approach* (New York: Springer)
[34] Godec A and Metzler R 2016 *Phys. Rev.* X **6** 041037
[35] Berg T 2008 *Curr. Opin. Chem. Biol.* **12** 464
[36] Majmudar C and Mapp A 2005 *Curr. Opin. Chem. Biol.* **9** 467
[37] Dix J A and Verkman A S 2008 *Annu. Rev. Biophys.* **37** 247

[38] Luby-Phelps K 2000 *Int. Rev. Cytol.* **192** 189
Chin D and Means A R 2000 *Trends Cell Biol.* **10** 322
[39] Goldstein R E and van de Meent J-W 2015 *Interface Focus* **5** 20150030
Reverey J F 2015 *Sci. Rep.* **5** 11690
[40] Viccario G, Antoine C and Talbot J 2015 *Phys. Rev. Lett.* **115** 240601
Cherstvy A G, Chechkin A V and Metzler R 2014 *J. Phys. A: Math. Theor.* **47** 485002
Cherstvy A G and Metzler R 2014 *Phys. Rev.* E **90** 012134
[41] Sabhapandit S, Majumdar S N and Comtet A 2006 *Phys. Rev. E* **73** 051102
Majumdar S N and Comtet A 2002 *Phys. Rev. Lett.* **89** 060601
Burov S and Barkai E 2007 *Phys. Rev. Lett.* **98** 250601
Dean D S. Gupta S. Oshanin G. Rosso A and Schehr G 2014 *J. Phys. A: Math. Theor.* **47** 372001
Bouchaud J-P and Georges A 1990 *Phys. Rep.* **195** 127
Krüsemann H, Godec A and Metzler R 2014 *Phys. Rev. E* **89** 040101
Krüsemann H, Godec A and Metzler R 2015 *J. Phys. A: Math. Theor.* **48** 285001
Godec A, Chechkin A V, Barkai E, Kantz H and Metzler R 2014 *J. Phys. A: Math. Theor.* **47** 492002
[42] Godec A, Bauer M and Metzler R 2014 *New J. Phys.* **16** 092002
[43] Barkai E, Garini Y and Metzler R 2012 *Phys. Today* **65** 29
Metzler R, Jeon J-H, Cherstvy A G and Barkai E 2014 *Phys. Chem. Chem. Phys.* **16** 24128
Höfling F and Franosch T 2013 *Rep. Prog. Phys.* **76** 046602
Jeon J-H *et al* 2011 *Phys. Rev. Lett.* **106** 048103
Bronstein I *et al* 2009 *Phys. Rev. Lett.* **103** 018102
Di Rienzo *et al* 2014 *Nat. Commun.* **5** 5891
Metzler R, Jeon J-H and Cherstvy A G 2016 *Biochim. Biophys. Acta* **1858** 2451